

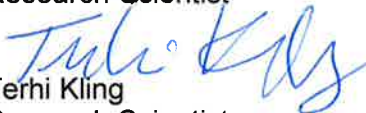





Fire defence-in-depth assessment in TVO cable room – feasibility study

Authors: Antti Paajanen, Terhi Kling

Confidentiality: Public

Report's title	
Fire defence-in-depth assessment in TVO cable room – feasibility study	
Customer, contact person, address	Order reference
SAFIR2014	
Project name	Project number/Short name
Risk Assessment of Large Fire Loads (LARGO)	73659/LARGO 2012
Author(s)	Pages
Antti Paajanen, Terhi Kling	34
Keywords	Report identification code
defence in depth, fire resistance, nuclear safety, fire simulation	VTT-R-01072-13
Summary	
<p>Part of the defence-in-depth assessment is the evaluation of the fire barrier performance. In this work, a simulation-based method is proposed for the barrier evaluation. The proposed approach is based on two central concepts: performance curves of barrier components and natural fire curves of compartment-specific fire-exposures.</p> <p>The performance curves are relatively simple, analytical time-temperature curves describing the thermal environment in a more realistic way than the standard fire curve. The performance of a barrier component under the exposure defined by the performance curve is determined using experimentally calibrated and validated computational models. The natural fire curves in turn represent realistic, compartment-specific, fire-exposures. They are acquired from stochastic fire simulations. The performance of a barrier component in a particular compartment can be assessed by comparing the two families of time-temperature curves.</p> <p>The feasibility of the method was here investigated using stochastic fire simulations in a nuclear power plant cable room. Natural fire curves were determined for cable penetrations, fire dampers and steel doors and compared with an example performance curve. Different types of thermal exposures were observed in the simulations. The example performance curve was found to envelope most of the simulated fire exposures but some problematic situations were also encountered. In these situations, the most severe thermal exposure reached a barrier after several hours of pre-heating at lower temperatures. The analytical form adopted for the performance curve was unsuitable for these situations. The performance of typical barrier components under these kinds of exposures is not well understood.</p>	
Confidentiality	Public
Espoo 8.2.2013	
Written by	Reviewed by
 Antti Paajanen Research Scientist	 Simo Hostikka Principal Scientist, Team Leader
 Terhi Kling Research Scientist	Accepted by  Eila Lehmus Technology Manager
VTT's contact address	
Antti Paajanen, Kemistintie 3, PL 1000 02044 VTT	
Distribution (customer and VTT)	
SAFIR2014 TR8, LARGO ad hoc –group	
<p><i>The use of the name of the VTT Technical Research Centre of Finland (VTT) in advertising or publication in part of this report is only permissible with written authorisation from the VTT Technical Research Centre of Finland.</i></p>	

Preface

This study was carried out as a part of the Risk Assessment of Large Fire Loads (LARGO) project which is one of the projects in the Finnish Research Programme on Nuclear Power Plant Safety (SAFIR2014). The study has been financed by the State Nuclear Waste Management Fund (VYR) and VTT Technical Research Centre of Finland.

Espoo 8.2.2013

Authors

Contents

Preface.....	3
Contents.....	4
1 Introduction.....	5
2 Evaluation of the fire compartmentation.....	6
2.1 General principle.....	6
2.2 Analytical form of the performance curve.....	7
2.3 Application example.....	7
3 Results and discussion.....	9
4 Conclusions.....	15
References.....	16
Appendix A: Details of the fire scenario.....	17
Appendix B: Details of the fire model.....	20
Appendix C: FDS material models.....	27

1 Introduction

The concept of “Defence in Depth” (DiD) or “independent protection layers” is a common approach for safety design in complex systems like chemical or nuclear plants or railway systems. To prevent and mitigate a system accident, several types of independent protective safety systems are installed to compensate a failure in some other protective system. INSAG-12 [1] describes the defence-in-depth principle in the following way: “To compensate for potential human and mechanical failures, a defence in depth concept is implemented, centred on several levels of protection including successive barriers preventing the release of radioactive material to the environment. The concept includes protection of the barriers by averting damage to the plant and to the barriers themselves. It includes further measures to protect the public and the environment from harm in case these barriers are not fully effective.”

One of the goals of the “Risk Assessment of Large Fire Loads” (LARGO) –project, is the development of methods for the evaluation of fire defence in depth. In the 2011 report [2], we introduced the methodology combining traditional event-tree analysis of the fire development and simulation-based evaluation of the fire resistance performance of partitioning elements. We acknowledge the fact that DiD means or can be understood to cover a range of different means to reduce the risk of severe accident. The internal layers of safety can be understood as consecutive physical barriers or sequential actions, referring to passive and active measures, respectively. The focus of the DiD evaluation in LARGO –project is in the evaluation of the physical barriers’ capability to protect the neighbouring spaces from a fire.

In this report, we investigate the feasibility of the proposed methodology in the light of the simulated fires in the cable room of the Olkiluoto nuclear power plant. This particular room may not be most urgent application of the defence-in-depth assessment. It is used here as an example because the fires in this room have been investigated by thorough numerical simulations in the past. The results of these simulations have been reported in [3]. These simulations are here utilized as a starting point to generate a representative group of compartment specific but typical time-temperature curves. These curves are used to evaluate how many different types of the analytical fire performance curves will be needed in the real DiD assessment studies.

2 Evaluation of the fire compartmentation

2.1 General principle

To support the evaluation of fire defence-in-depth (DID), a new method for the assessment of the performance of passive fire barriers is suggested. According to codes and requirements, fire-separating building elements and associated equipment and fittings must be made so that the spread of fire from one compartment to another within a specified period of time will be prevented. The fire rating of a barrier is traditionally determined by the time it can withstand the standard fire curve (i.e. ISO 834). However, using the fire rating in the evaluation of compartmentation has an evident problem: Fire ratings based on the ISO 834 curve describe the performance of fire barriers in a very simple thermal environment which can be overly conservative or optimistic, depending on the case.

Based on the basic ideas of the EPRESSI-method [4], we suggest a new method that can be used to evaluate the performance of compartmentation in fires. The method is based on three main steps:

1. Determine performance curves for the barrier component

Experimentally calibrated and validated computational models are used to forecast the behaviour of fire barriers or barrier components with boundary conditions given by time-temperature curves that describe the thermal environment in a more realistic way than the standard fire curve. These performance curves represent the conditions that the fire barrier can withstand. The evaluation of the performance requires pre-defined acceptance criteria. These criteria can be similar to those used in the context of experimental testing of building elements, such as a requirement for the mean and maximum temperature rise, or set by the limiting conditions tolerated by the neighbouring compartment or its contents.

2. Determine natural, compartment-specific, fire-exposures

Time-temperature curves representing natural (realistic) fire-exposures are determined based on stochastic fire simulations. These can include tens or even hundreds of simulated fires.

3. Compare the performance curves with the simulated fire-exposures.

The barrier is assumed to withstand a fire in the compartment if any of the performance curves envelops the simulated time-temperature curve. The probability of successful compartmentation is calculated as a fraction of simulated fire curves for which the above condition is true.

The comparison of simulated temperatures and prescribed performance curves requires consistent determination of the temperature from the fire simulation. For this purpose, the best suited quantity is so-called Adiabatic Surface Temperature T_{AST} which is defined as

$$\varepsilon_s (\dot{q}_{inc}'' - T_{AST}^4) + h_s (T_g - T_{AST}) = 0 \quad (1)$$

where ε_s is the surface emissivity, \dot{q}_{inc}'' is the incoming radiative heat flux, h_s is the convective heat transfer coefficient and T_g is the local gas temperature.

2.2 Analytical form of the performance curve

One way of defining a performance curve is given in Gautier et al. [4]. Gas temperature in the fire compartment during the spreading phase of a fire is given by

$$\theta_g = 20^\circ\text{C} + (1 - 0.324e^{-at} - 0.204e^{-bt} - 0.472e^{-ct}) \cdot 1325^\circ\text{C} \quad (2)$$

where t is the time from ignition in hours and a , b and c are numerical parameters. The decay phase begins when the spreading phase has reached a predefined duration t_1 . The linear decay phase is characterized by its slope β . After the temperature has decreased to a predefined value of T_2 , a final phase with constant temperature begins. Thus, the performance curve is defined by six parameters, namely a , b , c , β , t_1 and T_2 . The shape of the curve is shown in Figure 1 below.

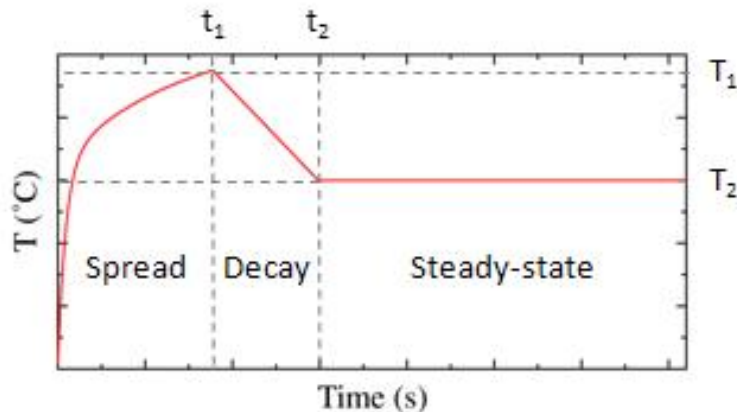


Figure 1. An example of a performance curve that is characterized by (i) spread, (ii) decay and (iii) steady-state phases.

2.3 Application example

The method is demonstrated using existing simulations of cable-originated fires in a cable room of the Olkiluoto I nuclear power plant (Figure 2) [5–7]. The primary fire load in the room is comprised of power and information cables. The information cables are enclosed in metal housings which are assumed to protect them from thermal and mechanical stresses and to reduce their potential heat release rate. The power cables are unprotected, and thus a more probable source of ignition. Both cable types are supported by a complex cable tray system. In the simulations, fire was assumed to ignite on the power cables of sub-system B. Originally, simulations were carried out both with and without the sprinkler system. Here, we only consider the case without sprinkler system as the sprinkler system efficiently prevented the growth of the fire.

The fire scenario was modelled using Fire Dynamics Simulator [8] (FDS). The model included all of the major objects and structures found in the cable room, i.e. the cable trays, mechanical screen plates, smoke collector plates, fire dampers, steel doors and the ventilation system. The source of ignition was given a random location on the power cables of sub-system B. A stochastic simulation of one hundred fires was performed. The fire scenario is described in more detail in Appendix A and the fire model in Appendix B.

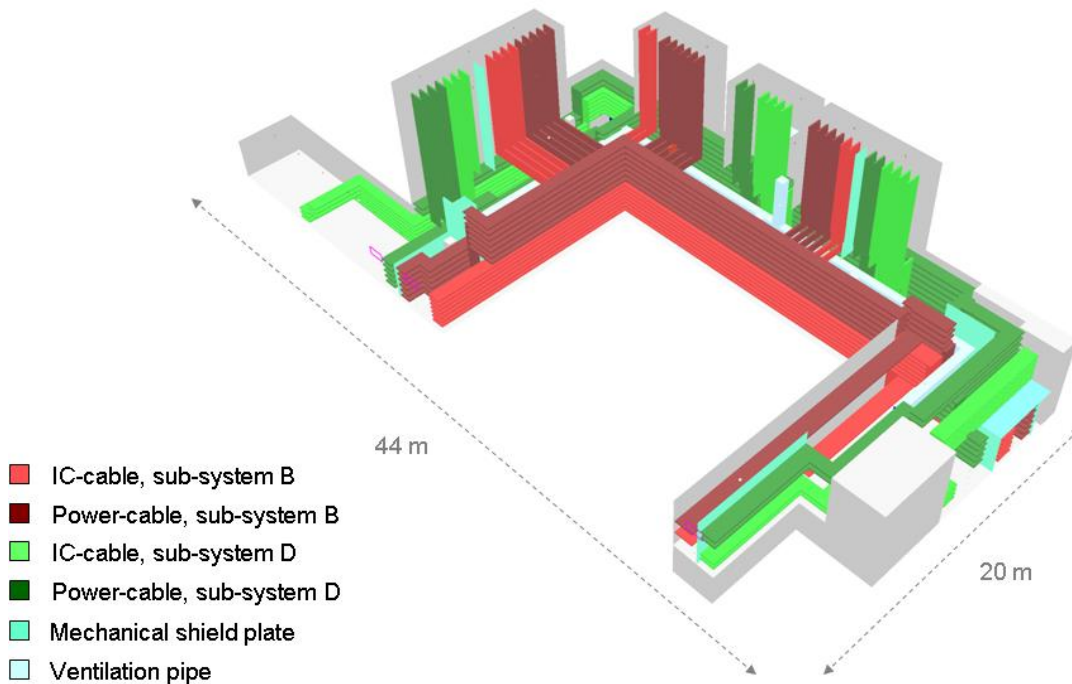


Figure 2. Computer visualization of the cable room. Cable trays are denoted by red and green colours. Mechanical shield plates are denoted by light blue colour, ventilation pipes and concrete structures by light grey colour.

Among the hundred fires without sprinklers, eight were chosen for further analysis. In each of them, the maximum heat release rate exceeded 10 MW. The simulation time was extended from one hour to four hours, and several measurement devices were added for monitoring the heating of barrier components at key locations (Figure 3). These include doors to neighbouring rooms, outflow vents and cable penetration seals.

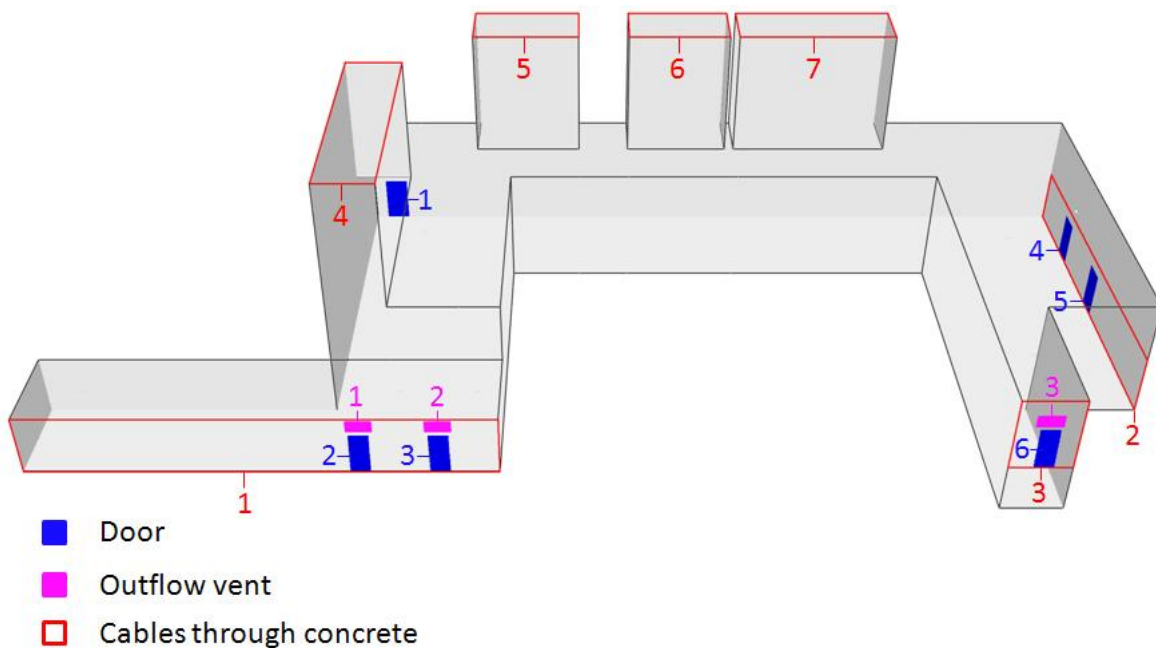


Figure 3. Measurement device set-up. Doors are denoted by blue and outflow vents by magenta colour. Wall areas with cable penetration seals are outlined in red. At each location, measurement devices were set up to monitor the maximum surface temperature and adiabatic surface temperature.

3 Results and discussion

The following parameterization was used to define the performance curve of the steel doors, the outflow vents and the cable penetration seals.

$$\{a, b, c, \beta, t_1, T_2\} = \{1.8, 15.0, 10.0, -300.0, 0.3737, 500.0\}$$

The choice of parameters is arbitrary and is only intended to serve demonstration purposes.

To monitor the fire temperature at the location of the target components (doors, fire dampers, cable penetrations), a single time-temperature curve for each location was determined by finding the maximum value over the surface of the corresponding components. Figure 4 shows the maximum AST curves from the eight simulations for each of the three fire dampers (vents 1-3). As can be seen, some of the eight simulations were still not finished at the time of writing this report. For vents 1 and 2, the performance curve (red curve) envelopes most of the simulated temperature curves. Among the eight fires, there is one fire that produces high temperatures at the location of these components only 10000 s from the ignition. Before that, the temperature grows steadily to a level of 200 °C. For Vent 2, the red performance curve captures the envelope of the two fires that produce high, almost 1000 °C temperatures early in the fire. For the Vent 3, the simulated temperatures exceed the performance curve during the decay phase. During the growth phase, the performance curve would be an overly conservative representation of the fire conditions. Similar conclusions can be made for the cable penetrations (Figure 5) and fire doors (Figure 6).

The nature of the simulated fires can be seen in the time-temperature curves of Figures 4–6. For some barrier components, high heat exposures are measured during the first 30 minutes. In these cases, the source of ignition was near the component, and the fire reached the component before the fire was affected by the local fuel burnout or lack of oxygen. For many barrier components, however, considerable peaks in heat exposure are observed after one to four hours from ignition. The heat exposure is characterized by an extended period of pre-heating in a few hundred degrees Celsius. This kind of behaviour is made possible by the large size and complicated geometry of the fire compartment and the distribution of the fire load. Figure 7 shows one example where the fire ignites close to the doors on the right but moves to the other end of the room in less than three hours. In fire literature, these fires are sometimes called ‘travelling fires’. Figure 8 shows the heat release rate curves of the fire simulations.

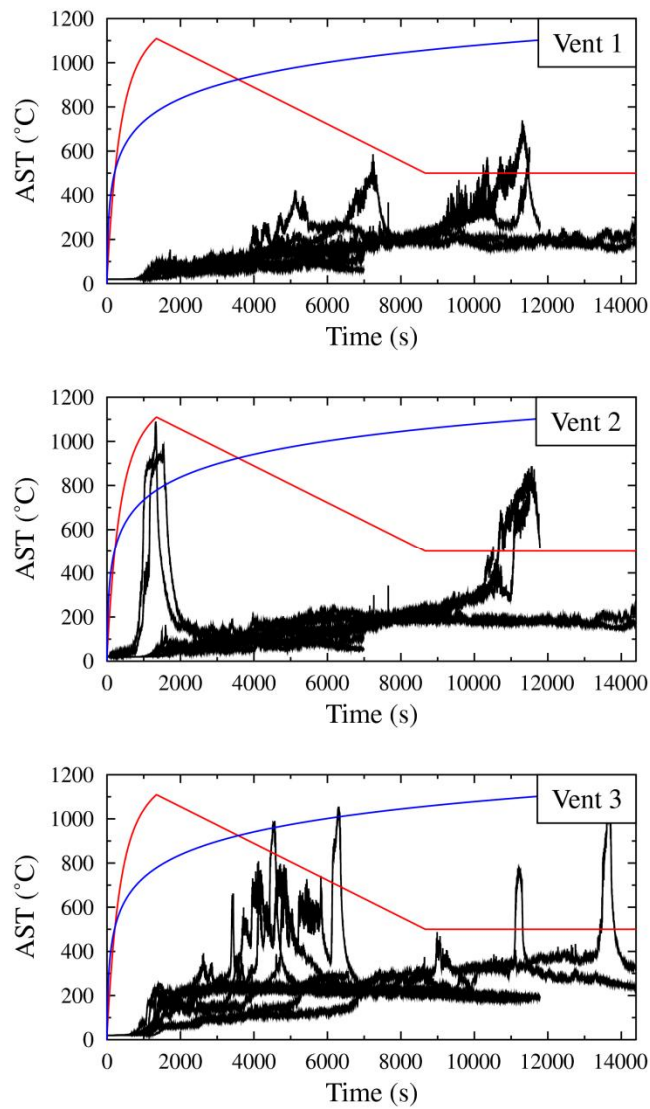


Figure 4. Maximum adiabatic surface temperature at the locations of the fire dampers. The performance curve is plotted in red colour and the standard fire curve in blue colour.

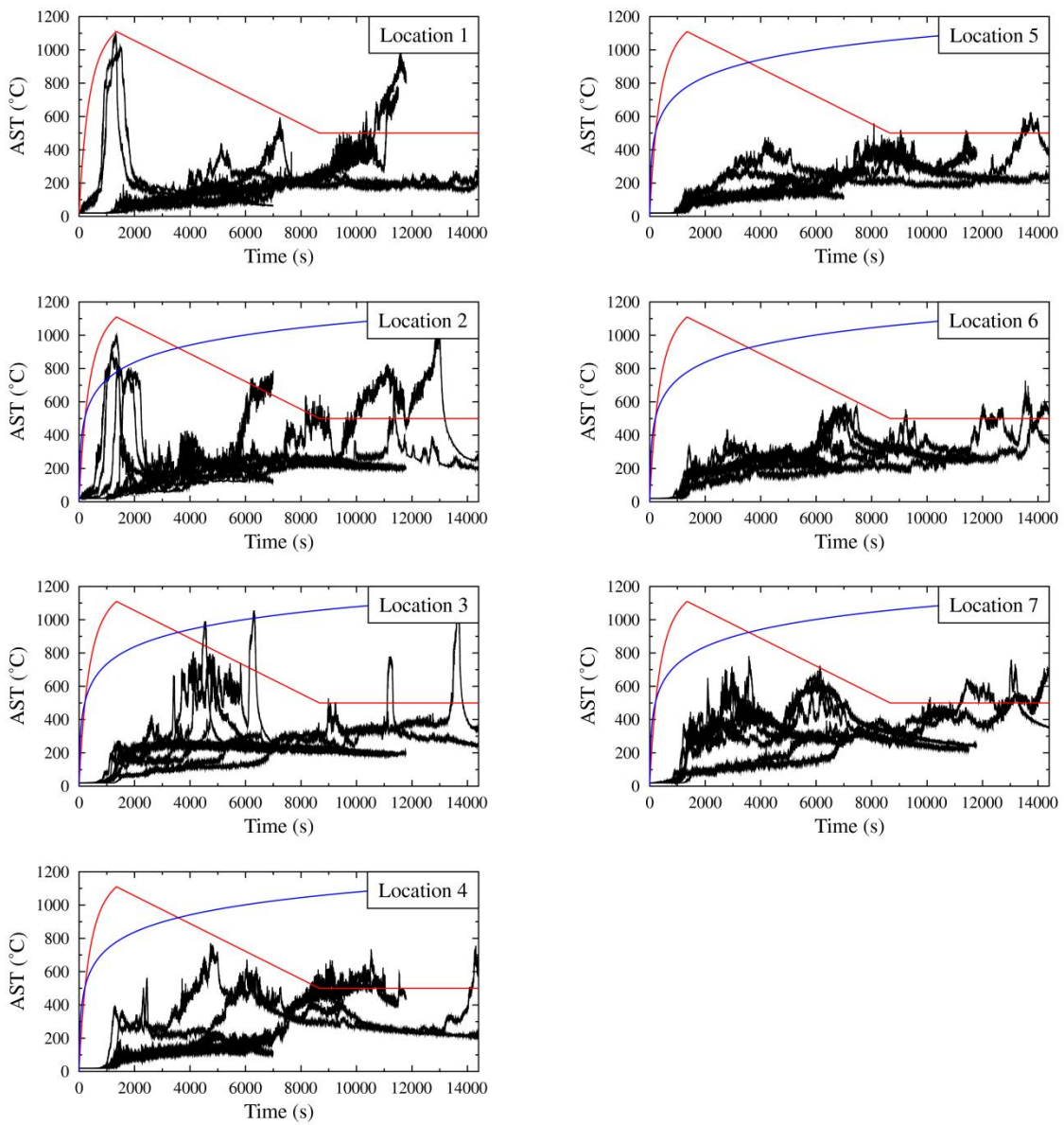


Figure 5. Maximum adiabatic surface temperature at the locations of the cable penetration seals. The performance curve is plotted in red colour and the standard fire curve in blue colour.

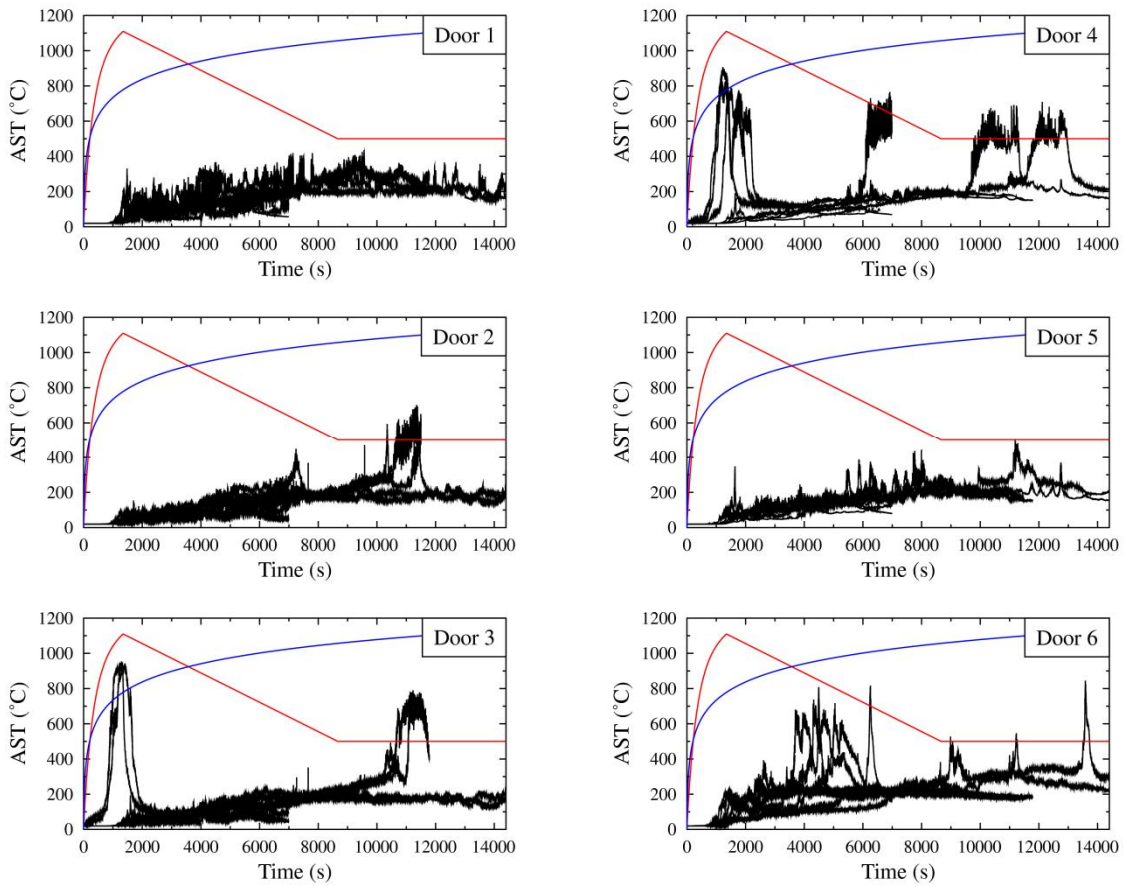


Figure 6. Maximum adiabatic surface temperature at the doors. The performance curve is plotted in red colour and the standard fire curve in blue colour.

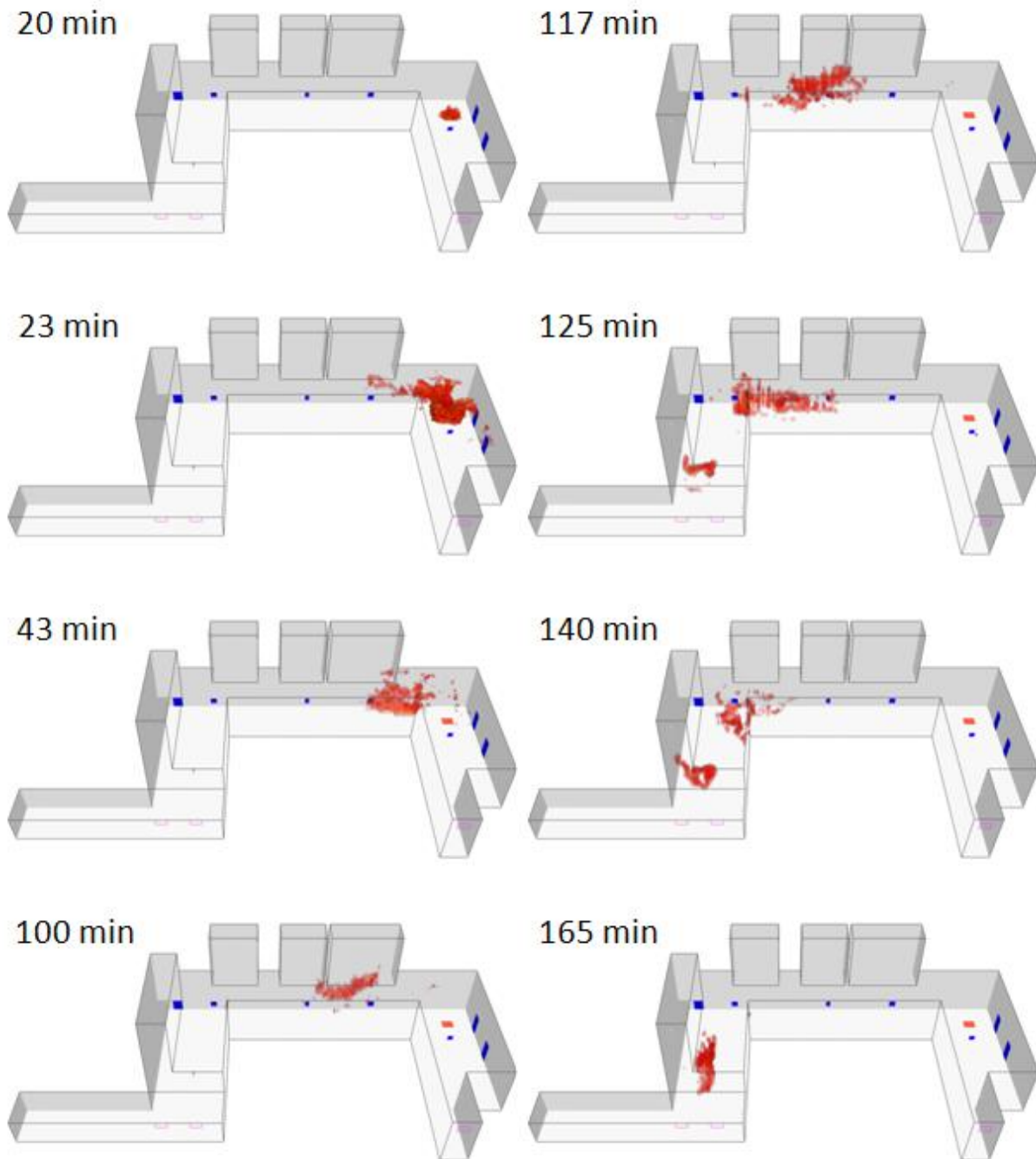


Figure 7. Location of the flame front in one of the simulations at several times from the ignition. The series of pictures illustrates the origin of the measured heat exposures.

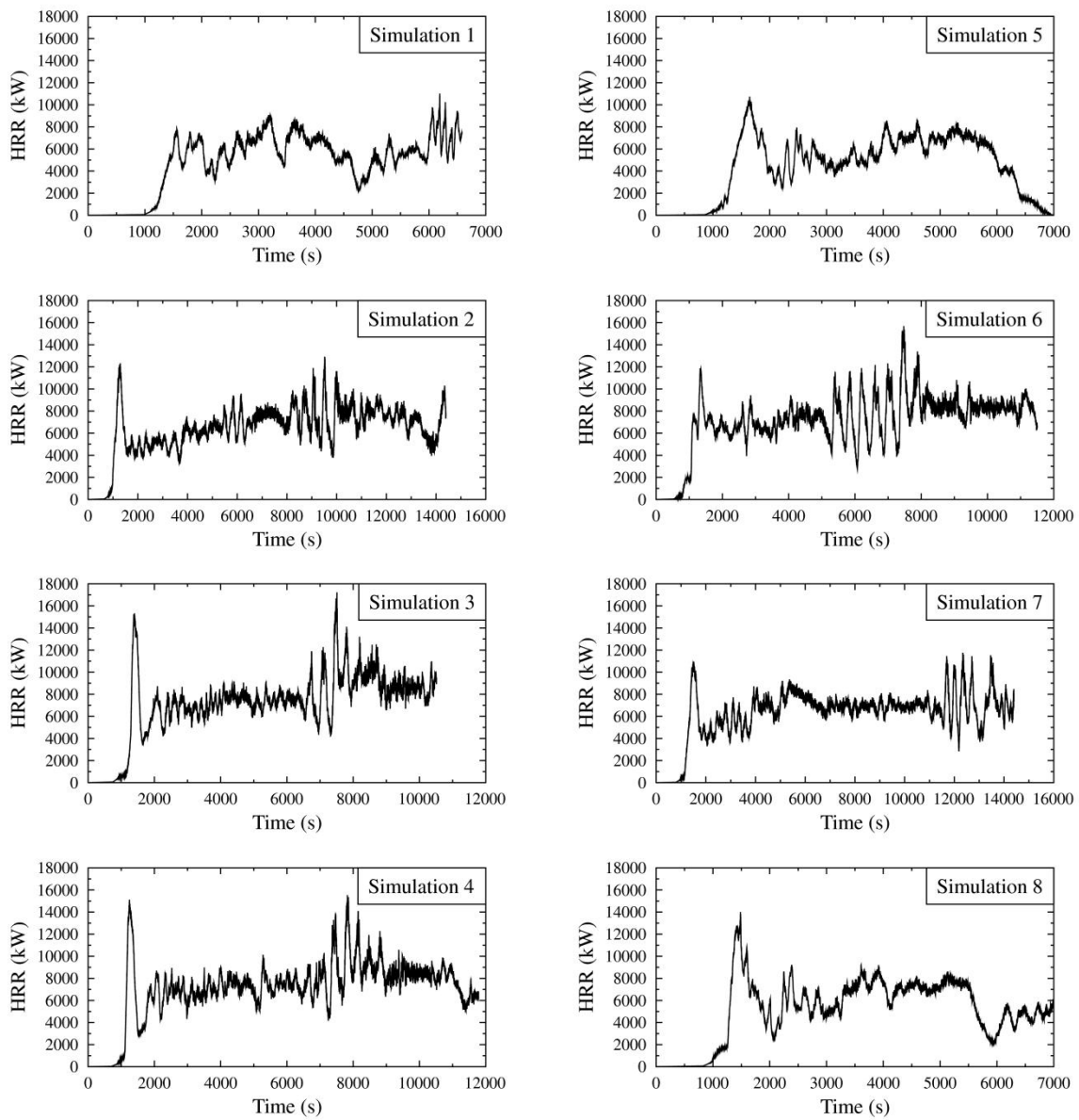


Figure 8. Net heat release rates in the fire simulations.

4 Conclusions

The feasibility of the modified EPRESSI –method for the characterization of the thermal environment in a compartment fire was investigated. Eight most severe fire realizations were chosen from a previous set of Monte Carlo simulations. These simulations were continued for an extended period of time to determine the four-hour exposure. Thermal exposures were collected at several locations of the large cable room in terms of the adiabatic surface temperature.

From the simulations, different types of fire exposures (test loads) were identified. Most of the observed temperature curves could be represented using the family of existing performance curves, but some new types of time-temperature curves were also found. These curves were results of fires that extended in space and time (travelling fires). In this kind of environment, the most severe thermal exposure might reach a certain fire barrier only after several hours of pre-heating at a few hundred degrees Celsius. The analytical form of the performance curve adopted for this study is unsuitable for these special situations. The performance of the typical barrier components under this kind of exposure is not well understood. These topics will be investigated in the future.

References

1. IAEA, 1999. Basic Safety Principles for Nuclear Power Plants. INSAG-12, 75-INSAG-3 Rev. 1, A report by the International Nuclear Safety Advisory Group, International Atomic Energy Agency, 1999.
2. T. Kling, S. Hostikka, Assessment of defence in depth in NPP fire safety. VTT Research Report VTT-R-00173-12. 10.2.2012.
3. T. Kling, S. Hostikka, A. Paajanen. Simulation of fire behaviour and human operations using a new stochastic operation time model. Proceedings of the 11th International Probabilistic Safety Assessment and Management Conference & The Annual European Safety and Reliability Conference. The International Association for Probabilistic Safety Assessment and Management (IAPSAM); 2012. The European Safety and Reliability Association (ESRA), 08-Mo3-1. PSAM11 & ESREL 2012. Helsinki, 25 - 29 June 2012.
4. B. Gautier, M. Mosse and O. Eynard, "EPRESSI Method – Justification of the Fire Partitioning Elements", Proc. Of the Sixth International Seminar on Fire & Explosion Hazards, 2011, pp. 374–385
5. S. Hostikka, "Probabilistic Fire Simulation of Cable Room", VTT Report VTT-R-01101-07, 2007
6. S. Hostikka, A. Matala and J. Mangs, "Probabilistic Fire Simulation of Cable Room – Preliminary Simulations of Cable-Originated Fires", Working report for the 2007 contribution to FIRAS task 2.1, 2008
7. A. Matala and S. Hostikka, "Probabilistic simulations of cable fires in a cable tunnel", VTT Report VTT-R-00836-10, 2010
8. National Institute of Standards and Technology, Gaithersburg, Maryland, USA, and VTT Technical Research Centre of Finland, Espoo, Finland, "Fire Dynamics Simulator, Technical Reference Guide", 5th edition, October 2007, NIST Special Publication 1018-5

Appendix A: Details of the fire scenario

Overview

The target of the analysis is a cable room in the Olkiluoto I nuclear power plant¹. A plan view of the room is shown in Figure A1. The room height is at most locations 5 m and at some locations 2.7 m (upper left and right wings in Figure A1). The room has four vertical cable shafts that reach to a height of 12 m above floor level. The walls, ceiling and floor are made of concrete. There are six entrances to the room through steel fire doors. A three-dimensional computer visualization of the room is shown in Figure A2.

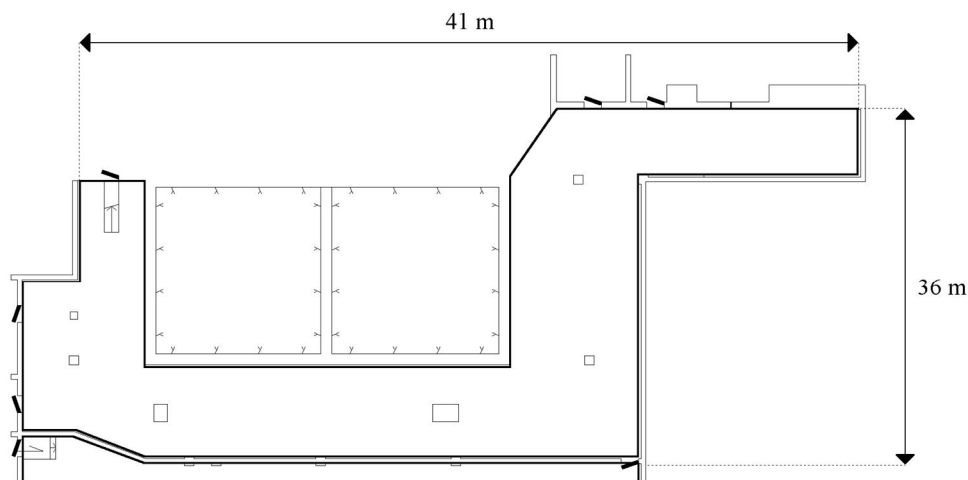


Figure A9. A plan view of the cable room

Fire load

The cable room contains power and IC-cables of two sub-systems (B and D). The cables are supported by a metallic cable tray system (Figure A3) that is designed to physically separate the two sub-systems where possible. Mechanical shield plates are installed between cable trays of the two sub-systems in locations where they come close to each other. The arrangement of the cable trays and the mechanical shield plates is shown in Figure A2. The exact amount of cabling is currently not known. A rough estimate is that the room contains about one kilometer of cable trays of both power and IC-cables.

Cables constitute the primary fire load found in the room. The IC-cables are, however, almost completely inside metal housings, which are assumed to both protect them from mechanical and thermal stresses and to reduce the potential heat release rate of the trays. The power cables, on the other hand, are unprotected. For cable-originated fires, the power cables are considered to be a more probable source of ignition than the IC-cables. In this study the fire source is assumed to locate on the power cables of sub-system B.

¹ TVO Olkiluoto Plant I, Auxiliary systems building (124H), Cable culvert B, D at level 2.0

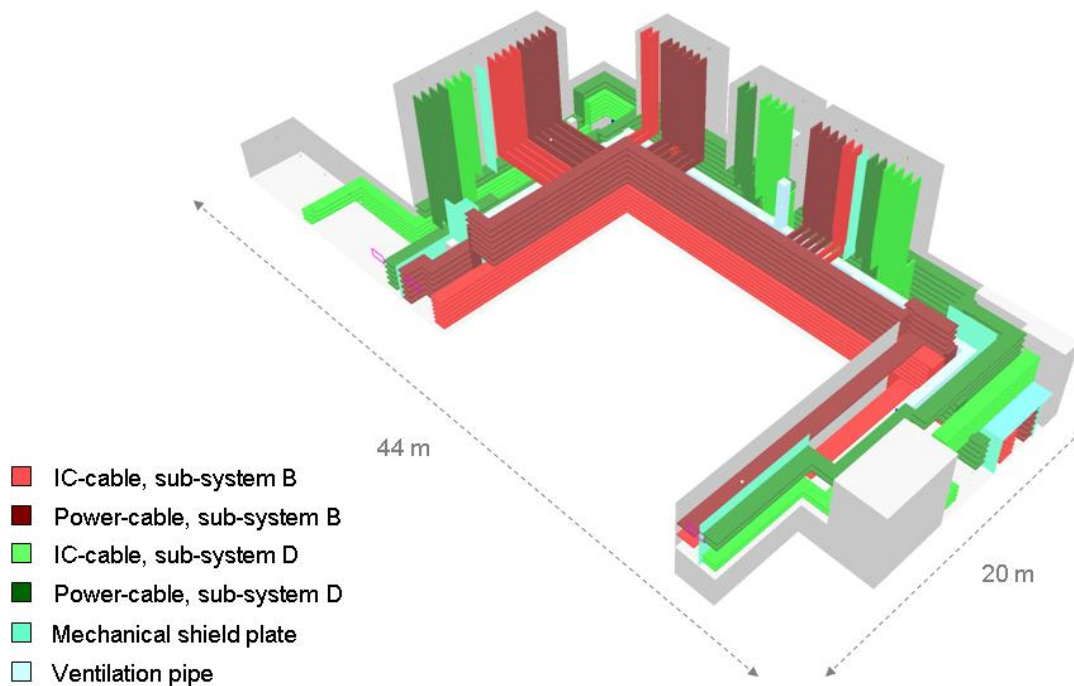


Figure A2. A computer visualization of the cable room. Cable trays of sub-system B are denoted by red colours and trays of sub-system D by green colours. Mechanical shield plates are denoted by light blue colour, ventilation pipes and concrete structures by light grey colour.



Figure A3. A photograph of part of the cable tray system. The eight lowest levels of cable trays (protected) contain IC-cables of sub-system B and the higher levels (unprotected) contain power cables of the same sub-system. Cable trays of sub-system D are located on the opposite side of the corridor (to the left in the picture).

Ventilation

The cable room has a mechanical ventilation system with a ventilation rate of 4000 l/s. Ventilation air is introduced from five terminals that are located at a height of 3 m above floor level. Exhaust air goes through three fire dampers that are located above doors to adjacent rooms. The locations of the ventilation pipes, air terminals and fire dampers are shown in Figure A4.

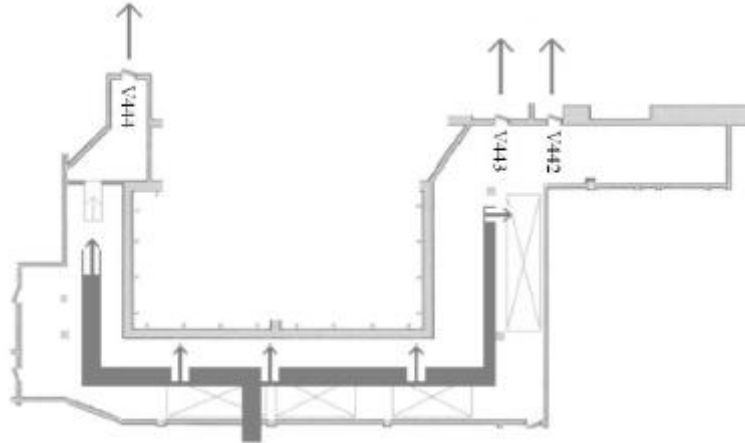


Figure A4. A schematic drawing of the ventilation system. Ventilation pipe is drawn in dark grey colour. The fire dampers are indicated by labels V442, V443 and V444. The ventilation pipe and the air terminals are located at a height of 3 m above floor level. (Figure by T.Purho, TVO)

Fire detectors

The room is equipped with 19 ESMI-2251-TEM combination smoke and heat detectors. Their operational principle is based on the simultaneous measurement of optical smoke density and temperature. The detectors are installed into the ceiling of the cable room and into the vertical cable shafts. In the shafts, the detectors are attached to horizontal steel plates to allow the collection of smoke around the detector heads.

Sprinklers

The cable room is equipped with a sprinkler system. However, in this study the system is assumed to be disabled.

Appendix B: Details of the fire model

The fire simulations were carried out using Fire Dynamics Simulator (FDS) (SVN revision 7595). FDS is a computational fluid dynamics program that contains models for fire-specific phenomena like combustion, thermal radiation, solid phase heat transfer and thermal degradation.

Simulation domain

For the purpose of the FDS simulation, the cable room was divided into nine rectangular computational meshes as shown in Figure B1.

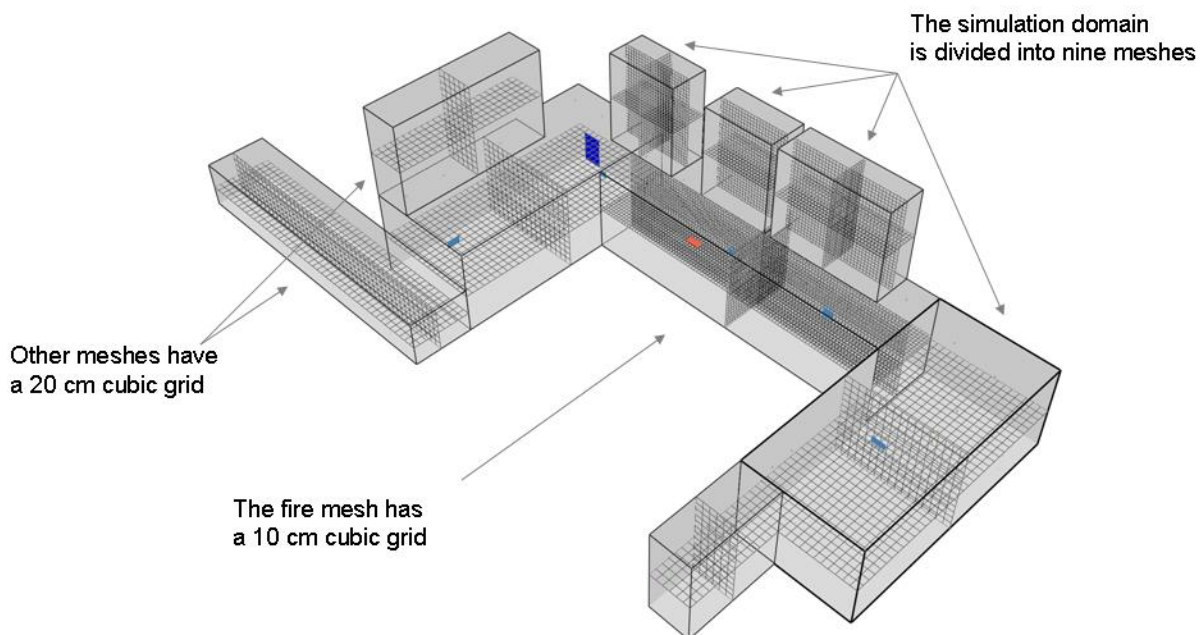


Figure B1. Computational meshes and grid resolution

Each mesh is divided into a number of rectangular cells that form a computational grid. The size of the cells defines the resolution of the flow dynamics calculation and the resolution at which objects and structures can be represented. Based on the results of a previous study [1] the grid resolution of the fire mesh (i.e. the mesh where the fire ignites) was selected to be 10 cm in all of the three spatial dimensions. To reduce the computational cost of the simulation, the resolution of other meshes was set to 20 cm. The coarser grid outside the fire mesh was considered adequate based on a grid sensitivity study. To improve the stability of the flow dynamics calculation, 40 cm gaps with no solid obstacles were introduced at inter-mesh boundaries.

The entire geometry of an FDS model is made up of rectangular objects. In this case the model includes all of the major objects and structures found in the cable room, i.e. the cable trays, mechanical shield plates, smoke collector plates, fire dampers, steel doors and the ventilation pipe. Additional concrete obstacles were defined to block parts of the meshes to mimic room shapes that were not captured by the mesh structure. Smoke detectors and measurement devices were modelled as point-like objects that have no effect on the flow dynamics. Examples of the representation of the cable room contents are shown in figures B2 and B3 (see also Figure A2). Colour coding is used to identify cable trays belonging to different sub-systems and different classes.

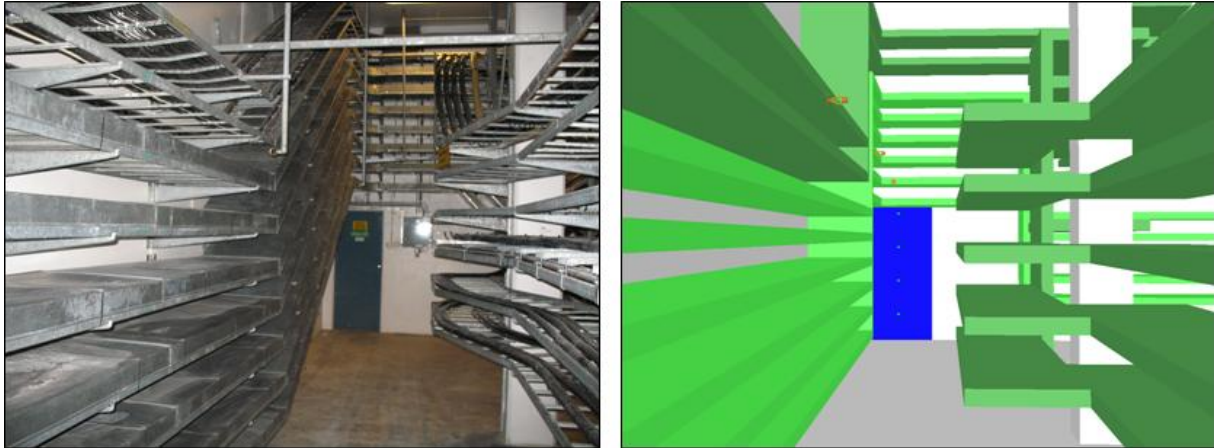


Figure B2. An example of the fire mesh resolution: a photograph from the cable room (left) and a computer visualization of the same location (right). Green colour denotes cable trays of sub-system D.

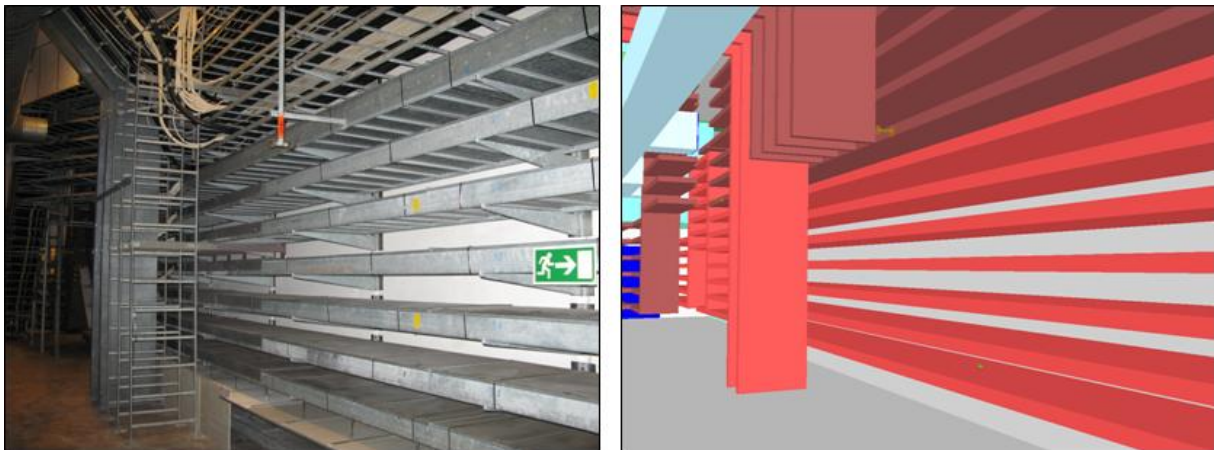


Figure B3. An example of the fire mesh resolution: a photograph from the cable room (left) and a computer visualization of the same location (right). Red colours denote cable trays of sub-system B.

Ventilation

The ventilation system was modelled according to the specifications given in Appendix A. Air inflow was assumed to be uniformly distributed between the five air terminals. The terminals were modelled as 0.5 m × 0.5 m rectangular vents that introduce air into the room at a rate of 800 l/s each. The fire dampers were modelled as 1.0 m × 0.5 m open vents. Closing of the fire dampers was not included in the model. Ambient air temperature was assumed to be 20°C.

Cable materials

The IC-cables are enclosed in cable conduits made of steel. The thickness of the conduit wall is 1 mm at the bottom and 2 mm on the sides and top. The IC-cables were modelled as one-sided² surfaces with 1 mm of steel on the top and 10 mm of non-reacting PVC material under the steel and a perfectly insulated back side boundary condition. Thus, heat is conducted inside the cable but the materials do not undergo any degradation reactions. It is also assumed that the cables are in direct contact with the metal housing.

² Only one side of the surface interacts with the environment

The power cable model is based on experimental data of NK Cables MCMK 0.6/1 kV 4 x 1.5/1.5 mm² cable (Figure B4). For the purpose of this study, slight modifications to the original cable model were made.

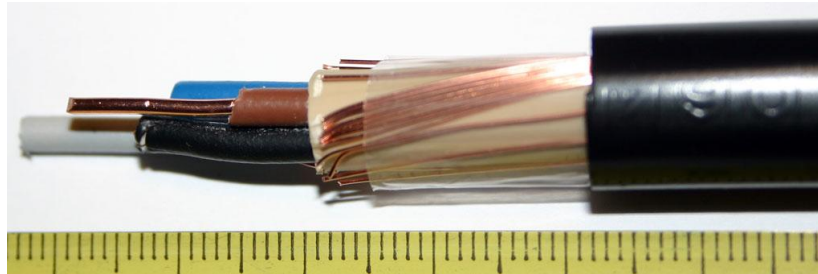


Figure B4. Cross-section of the NK Cables MCMK 0.6/1 kV 4 x 1.5/1.5 mm² cable

The power cables were modelled as two-sided surfaces with three homogeneous material layers. The layer structure is illustrated in Figure B5.

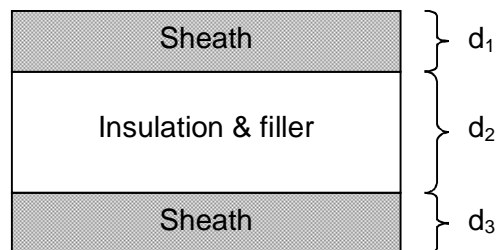


Figure B5. Layered structure of the power cable model (the metallic conductors are not included in the model). The thicknesses d_1 , d_2 and d_3 are defined as random variables in the stochastic simulation.

The material parameters of the IC-cable model are given in Table B1 and the general material parameters of the power cable model in Table B2. Pyrolysis-related parameters of the power cable model are given Appendix C (along with a complete description of the cable models).

Table B1. Material parameters of the constituents of the IC-cables (cable trays)

Material	Density (kg/m³)	Specific heat capacity (kJ/kg·K)	Thermal conductivity (W/m·K)	Emissivity
Steel	7850	0.46	45.8	0.9
PVC	1400	1.05	0.16	0.9

Table B2. General material parameters of the constituents of the power cables. Pyrolysis-related parameters are given in Appendix C.

Material	Density (kg/m³)	Specific heat capacity (kJ/kg·K)	Thermal conductivity (W/m·K)	Emissivity
Sheath 1	1316	2.00	-	1
Sheath 2	1316	2.09	-	1
Sheath 3	1316	2.80	-	1
Filler	1745	2.50	0.65	1
Insulation 1	1375	3.32	0.77	1
Insulation 2	1375	2.50	0.40	1

Other materials

Other materials include the material of the mechanical shield plates, the insulation material of the fire doors, concrete and steel. Their properties are listed in Table B3. Material properties of concrete were treated as random variables, and are therefore not given here.

Table B3. Properties of materials found in the cable room (excluding cable materials). The density, specific heat capacity and thermal conductivity of concrete are defined as random variables in the stochastic simulation.

Material	Density (kg/m³)	Specific heat capacity (kJ/kg·K)	Thermal conductivity (W/m·K)	Emissivity
Concrete	-	-	-	0.9
Steel	7850	0.46	45.8	0.9
Shield plate	1440	0.84	0.48	0.9
Insulation	300	2.00	0.05	0.9

Ignition and combustion

The source of ignition was assumed to be a burning power cable of sub-system B. The ignition source was implemented as a burner that envelopes a segment of one of the power cable trays. The time dependent heat release rate of the ignition source was adapted from a room scale experiment of PVC cable trays reported in [2]. A general form of the heat release rate curve is shown in Figure B6. The maximum heat release rate and the time of the maximum were defined as random variables in the stochastic simulation. The burner heat release rate per unit area was assumed to be 300 kW/m² and the area of the burner varied according to the maximum heat release rate.

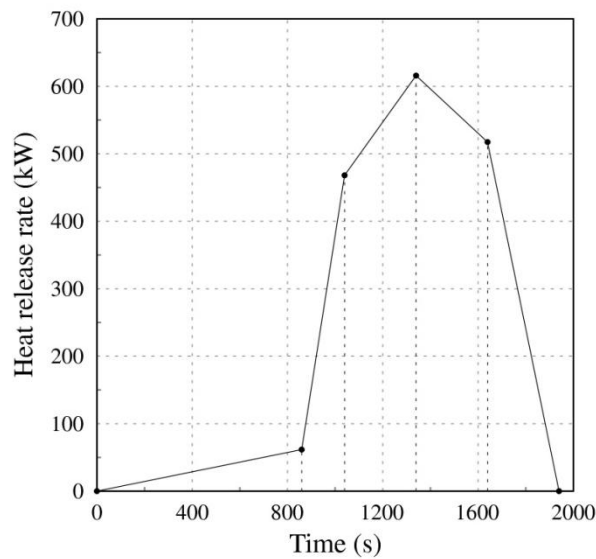


Figure B6. An example of the heat release rate curve of the source of ignition. The general form of the heat release rate curve is the same in all realizations.

The heat of combustion is assumed to be 40 MJ/kg which corresponds to the combustible part of the PVC material model. The radiative fraction of the combustion energy is set to 0.3. Mixture fraction model is used to describe the pyrolysis and combustion processes. A numerical limiter is used to limit the gas and solid temperatures above 19°C. The FDS parameters of the combustion reaction are given in Appendix C.

Stochastic simulation

The stochastic simulation consisted of one hundred FDS simulations of power cable –originated fires in the cable room. The simulations were set up according to the specifications given in the previous chapters. The simulation time was selected to be one hour. An additional stochastic simulation, where the sprinkler system was disabled, was also realized.

The random variables of the stochastic simulation were related to the size and location of the initial fire, the properties of the power cables and concrete and the response of the sprinkler system. The parameters of the probability distributions of the random variables are given in Table B4.

The location of the initial fire was selected at random (with a uniform probability distribution) from all possible locations on the power cables of sub-system B. The locations of the random initial fires are shown in Figure B7. The location of the fires was not part of the Latin hypercube sample formed by the other random variables.

Table B4. Properties of the random variables. Apart from the location of the initial fire, all random variables included in the stochastic simulation are listed above.

Variable	Symbol	Unit	Distribution	Minimum	Peak	Maximum
Maximum heat release rate of the initial fire	HRR_{max}	kW	Triangular	300	500	700
Time of maximum heat release rate	T_{peak}	s	Triangular	900	1200	1500
Specific heat capacity of concrete	C_p	kJ/kg·K	Uniform	0.6	-	1
Density of concrete	ρ	kg/m ³	Uniform	2100	-	2500
Thermal conductivity of concrete	k_c	W/m·K	Uniform	1.4	-	1.8
Thickness of cable sheath 1	d_1	mm	Uniform	2.184	-	3.276
Thickness of cable sheath 2	d_2	mm	Uniform	2.184	-	3.276
Thickness of cable insulation	d_i	mm	Uniform	2.56	-	3.84
Thermal conductivity coefficient of cable sheath material	α_k	-	Triangular	0.7	1	1.3
Response time index 1	RTI_1	(m·s) ^{1/2}	Triangular	120	150	180
Response time index 2	RTI_2	(m·s) ^{1/2}	Triangular	25	37.5	50
Activation temperature 1	T_1	°C	Triangular	67	74	81
Activation temperature 2	T_2	°C	Triangular	50	57	64

Origin of the probability distribution parameters

Probability distribution parameters of the maximum heat release rate of the source of ignition and the time of the maximum were adapted from a previous study [3]. The uniform probability distributions of concrete properties covered a range of values found in literature [4,5]. Thicknesses of the layers of the power cables were set to vary approximately 50% from those of the original NK Cables MCMK 0.6/1 kV 4 x 1.5/1.5 mm² cable model. The sprinkler activation parameters were set to vary slightly around the nominal values given by the manufacturers.

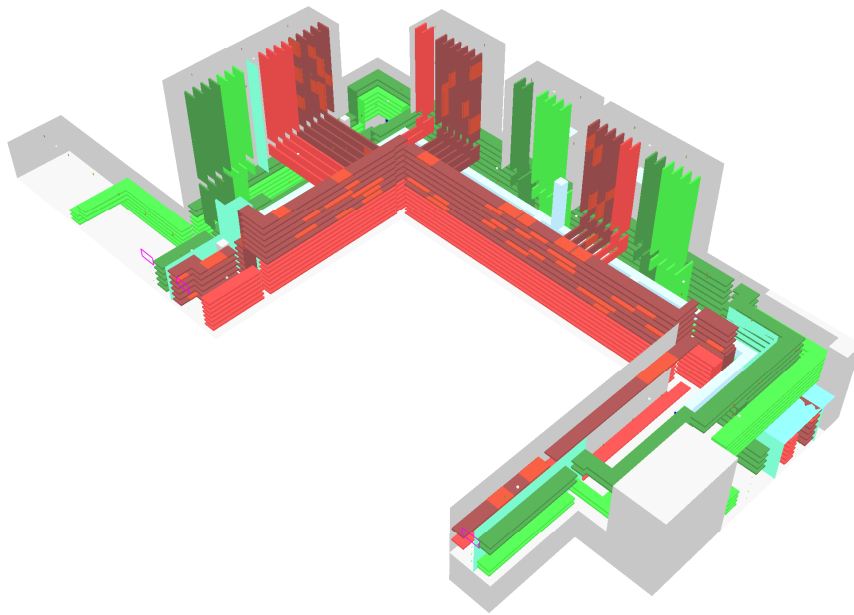


Figure B7. Locations of the random initial fires. The burners are denoted by red patches on the (dark red) power cables of sub-system B.

References

1. S. Hostikka, A. Matala and J. Mangs, "Probabilistic Fire Simulation of Cable Room – Preliminary Simulations of Cable-Originated Fires", Working report for the 2007 contribution to FIRAS task 2.1, 2008
2. J. Mangs and O. Keski-Rahkonen, "Full-scale fire experiments on vertical and horizontal cable trays", VTT publications 324, 1997
3. S. Hostikka, "Probabilistic Fire Simulation of Cable Room", VTT Report VTT-R-01101-07, 2007
4. N. Iwankiw, J. Beitel and R. Gewain, "Structural materials", Handbook of building materials for fire protection, Chapter 6, McGraw-Hill Handbooks, 2004
5. T.Z. Harmathy, "Properties of building materials", The SFPE Handbook of fire protection engineering, 2nd edition, Section 1, Chapter 10 and Appendix B, National Fire Protection Association, 1995

Appendix C: FDS material models

FDS input related to the cable models is given in what follows.

```

&SURF      ID=                'TARGET_B'
           RGB=                230, 75, 75
           BACKING=            'INSULATED'
           MATL_ID=            'STEEL', 'PVC_NONREAC'
           THICKNESS=          0.001, 0.01          /

&SURF      ID=                'TARGET_D'
           RGB=                75, 230, 75
           BACKING=            'INSULATED'
           MATL_ID=            'STEEL', 'PVC_NONREAC'
           THICKNESS=          0.001, 0.01          /

&SURF      ID=                'BSUB_POWER'
           RGB=                150, 75, 75
           LAYER_DIVIDE=       RANDOM VARIABLE
           BACKING=            'EXPOSED'
           MATL_ID(1,1)=       'SHEATH_V'
           MATL_ID(1,2)=       'SHEATH_S1'
           MATL_ID(1,3)=       'SHEATH_S2'
           MATL_MASS_FRACTION(1,:)= 0.56, 0.11, 0.33
           MATL_ID(2,1)=       'FILLER_1'
           MATL_ID(2,2)=       'INSULATION_V'
           MATL_ID(2,3)=       'INSULATION_S1'
           MATL_MASS_FRACTION(2,:)= 0.519, 0.238, 0.243
           MATL_ID(3,1)=       'SHEATH_V'
           MATL_ID(3,2)=       'SHEATH_S1'
           MATL_ID(3,3)=       'SHEATH_S2'
           MATL_MASS_FRACTION(3,:)= 0.56, 0.11, 0.33
           THICKNESS=          RANDOM VARIABLES      /

&SURF      ID=                'DSUB_POWER'
           RGB=                75, 150, 75
           LAYER_DIVIDE=       RANDOM VARIABLE
           BACKING=            'EXPOSED'
           MATL_ID(1,1)=       'SHEATH_V'
           MATL_ID(1,2)=       'SHEATH_S1'
           MATL_ID(1,3)=       'SHEATH_S2'
           MATL_MASS_FRACTION(1,:)= 0.56, 0.11, 0.33
           MATL_ID(2,1)=       'FILLER_1'
           MATL_ID(2,2)=       'INSULATION_V'
           MATL_ID(2,3)=       'INSULATION_S1'
           MATL_MASS_FRACTION(2,:)= 0.519, 0.238, 0.243
           MATL_ID(3,1)=       'SHEATH_V'
           MATL_ID(3,2)=       'SHEATH_S1'
           MATL_ID(3,3)=       'SHEATH_S2'
           MATL_MASS_FRACTION(3,:)= 0.56, 0.11, 0.33
           THICKNESS=          RANDOM VARIABLES      /

&MATL      ID=                'STEEL'
           SPECIFIC_HEAT=      0.46
           DENSITY=            7850
           CONDUCTIVITY=       45.8
           EMISSIVITY=         0.9          /
  
```

```

&MATL      ID=                'PVC_NONREAC'
            SPECIFIC_HEAT=    1.05
            DENSITY=          1400
            CONDUCTIVITY=     0.16
            EMISSIVITY=       0.9          /

&MATL      ID=                'SHEATH_V'                ! Sheath 1
            EMISSIVITY=       1
            DENSITY=          1316
            CONDUCTIVITY=     RANDOM VARIABLE * 0.25
            SPECIFIC_HEAT=    2
            N_REACTIONS=      1
            A=                 7.55E+13
            E=                 173355.32
            N_S=              0.96150467
            NU_RESIDUE=       0
            NU_FUEL=          0.35
            NU_WATER=         0
            HEAT_OF_REACTION=  800
            HEAT_OF_COMBUSTION= 40000      /

&MATL      ID=                'SHEATH_S1'              ! Sheath 2
            EMISSIVITY=       1
            DENSITY=          1316
            CONDUCTIVITY=     RANDOM VARIABLE * 0.15
            SPECIFIC_HEAT=    2.09
            N_REACTIONS=      1
            A=                 5.43E+11
            E=                 240016.49
            N_S=              2.4810335
            NU_RESIDUE=       0.30982939
            NU_FUEL=          0.69017061
            NU_WATER=         0
            RESIDUE=          'CHAR_S'
            HEAT_OF_REACTION=  700
            HEAT_OF_COMBUSTION= 40000      /

&MATL      ID=                'SHEATH_S2'              ! Sheath 3
            EMISSIVITY=       1
            DENSITY=          1316
            CONDUCTIVITY=     RANDOM VARIABLE * 0.15
            SPECIFIC_HEAT=    2.8
            N_REACTIONS=      1
            A=                 6.50E+19
            E=                 295200.95
            N_S=              2.7058254
            NU_RESIDUE=       0.67357295
            NU_FUEL=          0.32642705
            NU_WATER=         0, 0
            RESIDUE=          'CHAR_S'
            HEAT_OF_REACTION=  700
            HEAT_OF_COMBUSTION= 45000      /
  
```

```

&MATL      ID=                'FILLER_1'
            EMISSIVITY=       1
            DENSITY=          1745
            CONDUCTIVITY=     0.65
            SPECIFIC_HEAT=    2.5
            N_REACTIONS=      1
            A=                 5.28E+09
            E=                 130862.15
            N_S=               0.7655183
            NU_RESIDUE=        0.75228809
            NU_FUEL=           0.24771191
            NU_WATER=          0
            RESIDUE=           'FILLER_2'
            HEAT_OF_REACTION=  800
            HEAT_OF_COMBUSTION= 30000      /

&MATL      ID=                'FILLER_2'
            EMISSIVITY=       1
            DENSITY=          1335
            CONDUCTIVITY=     0.45
            SPECIFIC_HEAT=    0.80536098
            N_REACTIONS=      1
            A=                 9.02E+07
            E=                 196996.42
            N_S=               2.4630699
            NU_RESIDUE=        0.5585782
            NU_FUEL=           0.4414218
            NU_WATER=          0
            RESIDUE=           'CHAR_F'
            HEAT_OF_REACTION=  300
            HEAT_OF_COMBUSTION= 40000      /

&MATL      ID=                'INSULATION_V'
            EMISSIVITY=       1
            DENSITY=          1375
            CONDUCTIVITY=     0.7667077
            SPECIFIC_HEAT=    3.3199064
            N_REACTIONS=      1
            A=                 1.77E+12
            E=                 150808.82
            N_S=               1.6872538
            NU_RESIDUE=        0
            NU_FUEL=           0
            NU_WATER=          0
            HEAT_OF_REACTION=  450      /

&MATL      ID=                'INSULATION_S1'
            EMISSIVITY=       1
            DENSITY=          1375
            CONDUCTIVITY=     0.4
            SPECIFIC_HEAT=    2.5
            N_REACTIONS=      1
            A=                 3.12E+14
            E=                 231594.19
            N_S=               3
            NU_RESIDUE=        0.75310722
            NU_FUEL=           0.24689278
            NU_WATER=          0
            RESIDUE=           'INSULATION_S2'
            HEAT_OF_REACTION=  300
            HEAT_OF_COMBUSTION= 45000      /
  
```

```
&MATL      ID=                'INSULATION_S2'  
           EMISSIVITY=       1  
           DENSITY=          1035  
           CONDUCTIVITY=     0.79415741  
           SPECIFIC_HEAT=    0.8  
           N_REACTIONS=      1  
           A=                1608248.5  
           E=                158942.5  
           N_S=              2.6209743  
           NU_RESIDUE=       0.76681247  
           NU_FUEL=          0.23318753  
           NU_WATER=         0  
           RESIDUE=          'CHAR_I'  
           HEAT_OF_REACTION= 300  
           HEAT_OF_COMBUSTION= 40000      /
```

```
&MATL      ID=                'CHAR_S'  
           EMISSIVITY=       1  
           DENSITY=          337  
           CONDUCTIVITY=     0.9  
           SPECIFIC_HEAT=    2          /
```

```
&MATL      ID=                'CHAR_F'  
           EMISSIVITY=       1  
           DENSITY=          745  
           CONDUCTIVITY=     0.25331522  
           SPECIFIC_HEAT=    1.2946197  /
```

```
&MATL      ID=                'CHAR_I'  
           EMISSIVITY=       1  
           DENSITY=          780  
           CONDUCTIVITY=     0.6669574  
           SPECIFIC_HEAT=    1.2941529  /
```

FDS input related to the cable models is given in what follows.

```
&SURF      ID=                'TARGET_B'  
           RGB=              230, 75, 75  
           BACKING=          'INSULATED'  
           MATL_ID=          'STEEL', 'PVC_NONREAC'  
           THICKNESS=       0.001, 0.01      /
```

```
&SURF      ID=                'TARGET_D'  
           RGB=              75, 230, 75  
           BACKING=          'INSULATED'  
           MATL_ID=          'STEEL', 'PVC_NONREAC'  
           THICKNESS=       0.001, 0.01      /
```

```

&SURF      ID=                'BSUB_POWER'
           RGB=                150, 75, 75
           LAYER_DIVIDE=      RANDOM VARIABLE
           BACKING=           'EXPOSED'
           MATL_ID(1,1)=      'SHEATH_V'
           MATL_ID(1,2)=      'SHEATH_S1'
           MATL_ID(1,3)=      'SHEATH_S2'
           MATL_MASS_FRACTION(1,:)= 0.56, 0.11, 0.33
           MATL_ID(2,1)=      'FILLER_1'
           MATL_ID(2,2)=      'INSULATION_V'
           MATL_ID(2,3)=      'INSULATION_S1'
           MATL_MASS_FRACTION(2,:)= 0.519, 0.238, 0.243
           MATL_ID(3,1)=      'SHEATH_V'
           MATL_ID(3,2)=      'SHEATH_S1'
           MATL_ID(3,3)=      'SHEATH_S2'
           MATL_MASS_FRACTION(3,:)= 0.56, 0.11, 0.33
           THICKNESS=        RANDOM VARIABLES /

&SURF      ID=                'DSUB_POWER'
           RGB=                75, 150, 75
           LAYER_DIVIDE=      RANDOM VARIABLE
           BACKING=           'EXPOSED'
           MATL_ID(1,1)=      'SHEATH_V'
           MATL_ID(1,2)=      'SHEATH_S1'
           MATL_ID(1,3)=      'SHEATH_S2'
           MATL_MASS_FRACTION(1,:)= 0.56, 0.11, 0.33
           MATL_ID(2,1)=      'FILLER_1'
           MATL_ID(2,2)=      'INSULATION_V'
           MATL_ID(2,3)=      'INSULATION_S1'
           MATL_MASS_FRACTION(2,:)= 0.519, 0.238, 0.243
           MATL_ID(3,1)=      'SHEATH_V'
           MATL_ID(3,2)=      'SHEATH_S1'
           MATL_ID(3,3)=      'SHEATH_S2'
           MATL_MASS_FRACTION(3,:)= 0.56, 0.11, 0.33
           THICKNESS=        RANDOM VARIABLES /

&MATL      ID=                'STEEL'
           SPECIFIC_HEAT=      0.46
           DENSITY=            7850
           CONDUCTIVITY=       45.8
           EMISSIVITY=         0.9 /

&MATL      ID=                'PVC_NONREAC'
           SPECIFIC_HEAT=      1.05
           DENSITY=            1400
           CONDUCTIVITY=       0.16
           EMISSIVITY=         0.9 /

&MATL      ID=                'SHEATH_V'                ! Sheath 1
           EMISSIVITY=         1
           DENSITY=            1316
           CONDUCTIVITY=       RANDOM VARIABLE * 0.25
           SPECIFIC_HEAT=      2
           N_REACTIONS=        1
           A=                  7.55E+13
           E=                  173355.32
           N_S=                0.96150467
           NU_RESIDUE=         0
           NU_FUEL=             0.35
           NU_WATER=           0
           HEAT_OF_REACTION=    800
  
```



```

HEAT_OF_COMBUSTION= 40000 /

&MATL ID= 'SHEATH_S1' ! Sheath 2
EMISSION= 1
DENSITY= 1316
CONDUCTIVITY= RANDOM VARIABLE * 0.15
SPECIFIC_HEAT= 2.09
N_REACTIONS= 1
A= 5.43E+11
E= 240016.49
N_S= 2.4810335
NU_RESIDUE= 0.30982939
NU_FUEL= 0.69017061
NU_WATER= 0
RESIDUE= 'CHAR_S'
HEAT_OF_REACTION= 700
HEAT_OF_COMBUSTION= 40000 /

&MATL ID= 'SHEATH_S2' ! Sheath 3
EMISSION= 1
DENSITY= 1316
CONDUCTIVITY= RANDOM VARIABLE * 0.15
SPECIFIC_HEAT= 2.8
N_REACTIONS= 1
A= 6.50E+19
E= 295200.95
N_S= 2.7058254
NU_RESIDUE= 0.67357295
NU_FUEL= 0.32642705
NU_WATER= 0, 0
RESIDUE= 'CHAR_S'
HEAT_OF_REACTION= 700
HEAT_OF_COMBUSTION= 45000 /

&MATL ID= 'FILLER_1'
EMISSION= 1
DENSITY= 1745
CONDUCTIVITY= 0.65
SPECIFIC_HEAT= 2.5
N_REACTIONS= 1
A= 5.28E+09
E= 130862.15
N_S= 0.7655183
NU_RESIDUE= 0.75228809
NU_FUEL= 0.24771191
NU_WATER= 0
RESIDUE= 'FILLER_2'
HEAT_OF_REACTION= 800
HEAT_OF_COMBUSTION= 30000 /

&MATL ID= 'FILLER_2'
EMISSION= 1
DENSITY= 1335
CONDUCTIVITY= 0.45
SPECIFIC_HEAT= 0.80536098
N_REACTIONS= 1
A= 9.02E+07
E= 196996.42
N_S= 2.4630699
NU_RESIDUE= 0.5585782
NU_FUEL= 0.4414218
NU_WATER= 0
RESIDUE= 'CHAR_F'
    
```

```

HEAT_OF_REACTION= 300
HEAT_OF_COMBUSTION= 40000 /
&MATL ID= 'INSULATION_V'
EMISSION= 1
DENSITY= 1375
CONDUCTIVITY= 0.7667077
SPECIFIC_HEAT= 3.3199064
N_REACTIONS= 1
A= 1.77E+12
E= 150808.82
N_S= 1.6872538
NU_RESIDUE= 0
NU_FUEL= 0
NU_WATER= 0
HEAT_OF_REACTION= 450 /

&MATL ID= 'INSULATION_S1'
EMISSION= 1
DENSITY= 1375
CONDUCTIVITY= 0.4
SPECIFIC_HEAT= 2.5
N_REACTIONS= 1
A= 3.12E+14
E= 231594.19
N_S= 3
NU_RESIDUE= 0.75310722
NU_FUEL= 0.24689278
NU_WATER= 0
RESIDUE= 'INSULATION_S2'
HEAT_OF_REACTION= 300
HEAT_OF_COMBUSTION= 45000 /

&MATL ID= 'INSULATION_S2'
EMISSION= 1
DENSITY= 1035
CONDUCTIVITY= 0.79415741
SPECIFIC_HEAT= 0.8
N_REACTIONS= 1
A= 1608248.5
E= 158942.5
N_S= 2.6209743
NU_RESIDUE= 0.76681247
NU_FUEL= 0.23318753
NU_WATER= 0
RESIDUE= 'CHAR_I'
HEAT_OF_REACTION= 300
HEAT_OF_COMBUSTION= 40000 /

&MATL ID= 'CHAR_S'
EMISSION= 1
DENSITY= 337
CONDUCTIVITY= 0.9
SPECIFIC_HEAT= 2 /

&MATL ID= 'CHAR_F'
EMISSION= 1
DENSITY= 745
CONDUCTIVITY= 0.25331522
SPECIFIC_HEAT= 1.2946197 /

&MATL ID= 'CHAR_I'
EMISSION= 1
DENSITY= 780
    
```

```
CONDUCTIVITY=          0.6669574  
SPECIFIC_HEAT=        1.2941529  /
```

FDS input related to the combustion reaction is given in what follows.

```
&REAC      ID=                'CABLE_REAC'  
          SOOT_YIELD=          0.05  
          HEAT_OF_COMBUSTION=  40000  
          C=                    2  
          H=                    3          /
```

Finally, input related to miscellaneous simulation parameters is given here.

```
&MISC      SURF_DEFAULT=        'CONCRETE_DEFAULT'  
          ALLOW_UNDERSIDE_DROPLETS= .TRUE.  /
```